Criticality Assessment of Urban Water Distribution Systems

Thanh Tran (6125174)
Thunchanok Phutthaphaiboon (6141153)

September 29, 2025

1 Introduction

This report provides a criticality assessment of the modified EPANET Net 2 water distribution system for the South Central Connecticut Regional Water Authority on the Cherry Hill/Brushy Plains area in the US. We first analyze the baseline network performance over a 5-day simulation, then identify and explain network vulnerabilities under three distinct 3-hour fire event scenarios, each requiring an excess demand of 126 L/s. The report concludes with recommendations to enhance system resilience and reduce the identified vulnerabilities to meet the minimum required pressure of 30 PSI (ca. 2.1 bar) during a fire event.

2 Simulation and Analysis

2.1 Baseline Performance Analysis

2.1.1 Network Topology and Infrastructure Interaction

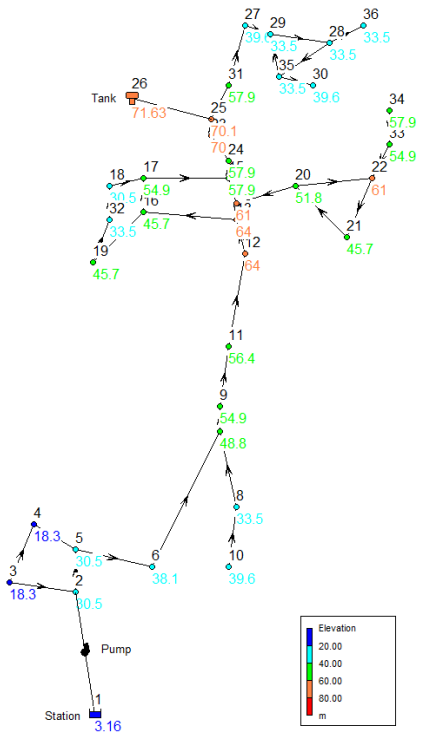

Figure 1: Infrastructure elevation

The system uses a combination of loops and branches.

The primary supply is driven by the reservoir (Node 1), which feeds the network through the pump station (Link 1). The pump is essential because the reservoir is at the lowest elevation (3.16 m) and the water must be actively pumped to overcome gravity and friction of the pipes to reach the significantly higher elevations of the northern area (see Fig 1). Thus, the pump here acts as a pressure booster to the system that helps deliver water downstream of the station. The tank (Node 26) is the crucial storage element, providing a backup water source and a pressure buffer.

The network's main vulnerability is the central branched line (nodes 6, 7, 9, 11, and 12). If a pipe breaks here, the entire upper part of the system loses its main water supply. This makes the tank (Node 26) extremely important for the north communities, as it releases stored water during peak demand or pump stops, keeping pressure steady and maintaining supply for that area. Additionally, the local looped sections (such as those near nodes 2-5 or 20-22) increase local reliability, since multiple paths allow water to be carried around a broken pipe.

2.1.2 Water Supply Fulfillment

Given the base demand of 20.41 L/s for all nodes of the system with regular demand multiplier (similar to the pattern in Fig 4, but without the demand peak at 67-69 hours), the current water supply (produced) is less than demand (consumed) as shown in the system flow balance (Fig 3).

The minimum required pressure of 30 PSI (ca. 2.1 bar) is equivalent to 21.42 meters of water head (mH2O), a unit used by the EPANET model where 1 bar is roughly 10 meters of head.

As seen in Fig 2, many nodes have pressures well below 30 PSI even during off-peak hours (left image, 14 nodes below 21.42 mH2O). During peak demand (right image), pressures drop drastically, with all 36 nodes below 21.42 mH2O and many exhibiting negative pressure, which indicates a fundamental supply failure in which the network cannot meet the required demand due to insufficient pressure.

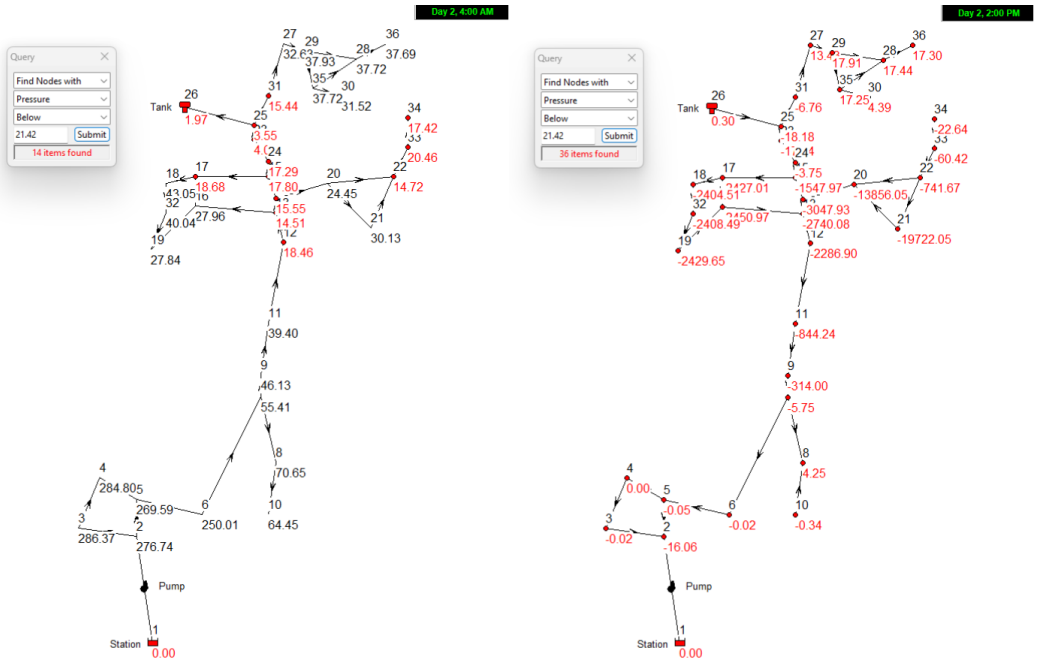

Figure 2: Comparison between off-peak (left) and peak (right) hours in baseline scenario

2.1.3 Vulnerability Period for Fire Event

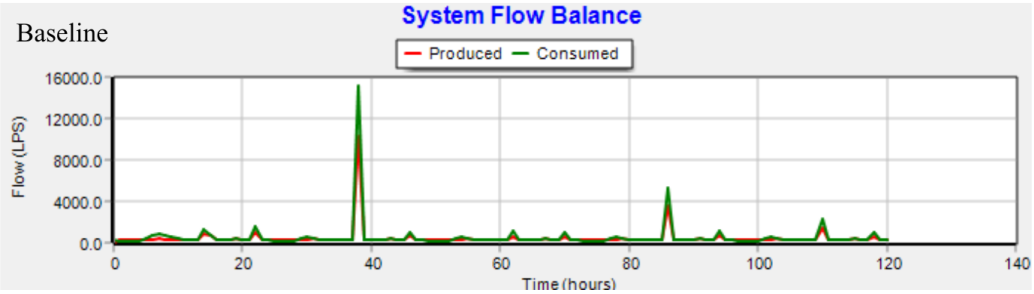

Figure 3: System flow balance of baseline scenario

The most vulnerable periods are expected to be around hour 39 and hour 87, as shown by the peaks in the "Consumed" flow in Fig 3 of the baseline scenario. These peaks indicate the times of maximum system demand. Adding the massive 126 L/s demand to mitigate the fire event at these moments will maximize the resulting pressure deficit and the number of nodes experiencing supply failure (vulnerability). However, if the fire event happens at a different time other than hour 39 and

87, it is expected that the vulnerability of the system will occur towards the end of the fire event where the tank level is the lowest and the friction losses peak.

2.2 Fire Event Simulation and Vulnerability Assessment

Three distinct 3-hour fire events are simulated, each adding a high excess demand of 126 L/s (around 20.41 L/s of base demand multiplied by 6.2) during hours 67–69 (see Fig 4) to test the network's resilience. Simulations for three fire events are conducted at different locations (a) fire at junction J5, (b) fire at junction J7, (c) wildfire control at J4 and J19.

Based on the earlier assumption, we examined the system's flow rate (L/s) and pressure (m) at hour 70 (Day 3, 10 PM), immediately following the wildfire event. As shown in the pressure map Fig A.2, many nodes experience pressures well below the minimum threshold of 21.42 m. This is because when a fire event happens, a large amount of water is pulled out of the system for several hours. This sudden extra flow makes it harder for water to move through the pipes, because higher flows create much more resistance. As a result, the pressure drops sharply along the pipes leading to the fire hydrant, and that drop can spread to other parts of the network. We define vulnerability at a node as the condition where the base demand (scaled by the demand pattern multiplier of 0.9 at hour 70) cannot be met and the available pressure falls below the minimum requirement of 21.42 m.

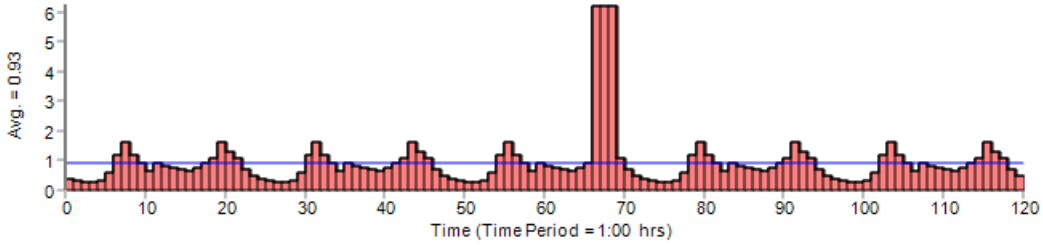

Figure 4: Water demand multiplier with a 3-hour fire event

2.2.1 Scenario A: Fire at junction 5

The fire event at J5 creates a significant demand surge at hour 70 (see Fig A.1), which is substantial when compared with the flow balance of the baseline (see Fig 3).

Table A (in Fig A.4) shows 26 junctions failing both criteria, spanning the central spine (J4–J9, J10-25) and eastern branch (J31–J34). Several exhibit very low or negative pressures, indicating localized isolation. At the same time, the tank pressure falls to 0.30 m, confirming system head is at its minimum. As seen in Fig A.3, the three-hour J5 fire (hours 67–69) produces the deepest trough, with maximum storage draw and minimum hydraulic grade near hour 69. This aligns with the hour-70 snapshot, where 26 junctions fall below both the 18.37 L/s demand (calculated by multiplying base demand and the normal demand multiplier of the 70H) and 21.42 m pressure thresholds.

Compared to baseline operation, the J5 fire event causes widespread deficits along the main conveyance path and downstream branches. The worst performance is driven by hydraulic depletion rather than diurnal peaks: after three hours of fire flow, the hydraulic grade line reaches its minimum at hour 70, when the system has not recovered. Several nodes show negative delivered demands, indicating back-feeding under severe stress.

2.2.2 Scenario B: Fire at junction 7

Unlike the immediate surge at hour 70 seen in Scenario A (See (A) in Fig A.1), the system flow balance for the wildfire event at J7 shows no notable difference from the baseline flow balance pattern in Fig 3.

At this step, 26 junctions fail both criteria (as shown in Table B in Fig A.4). The tank connection shows 0.30 m head, indicating near drawdown. The vulnerable nodes in this scenario are: J4–J9, J10-25, and J31–J34. However, it's worth noting that between J5 and J7 the ground rises by 18.3 m (30.5 to 48.8 m) as can be seen in Fig 1. With the tank at 71.63 m, the static heads are 41.1 m at J5 and 22.8 m at J7, leaving J7 only 1.4 m above the 21.42 m minimum before any friction losses. Under fire conditions, the lowered hydraulic grade line pushes J7 below the limit first (hr 70: J7 = -4.6 m,

J5 = +0.05 m in Fig A.4), confirming that the elevation step primarily governs pressure in this reach and makes J7 markedly more vulnerable than J5.

Additionally, it's noteworthy to point out that, as shown in both Fig A.1 and Fig A.3, the flow-balance plots reveal different supply mixes. With the fire at J5 (from 67–69 h), storage (or tank) carries much of the load, and a strong post-event refill spike appears as pumps recharge the tank. With the fire at J7 during the same hours, the pump/reservoir supplies most of the flow, tank draw is minor. That's why hours 67–69 show no distinctive surge. The tall spike near hour 36 in the J7 plot is routine tank cycling, not the fire. Overall, the tank functions primarily as a peaking/pressure buffer for the lower-elevation part of the system (around J5), while the pump–reservoir is the dominant supplier for higher-elevation nodes nearer J7.

2.2.3 Scenario C: Fire at junctions 4 and 19

Carrying the assumption that the network is most vulnerable at hour 70, we speculated the pressure and demand at this hour for 2 concurrent fire events happening at J4 and J19. It can be observed that there are more nodes that are impacted when these fire events occur than in the previous 2 scenarios. All nodes except for J8, J27, and J28 are vulnerable here. Pressures and water demand collapse along the central trunk and the eastern limb, with extreme deficits at J19 and downstream nodes (J20–J22 and J33–J34).

Table C in Fig A.4 best illustrates this worst moment, and it aligns with the time series plot D in Fig A.3: the tank outflow shows a clear dip during the 67–69 window, confirming storage participation during these 2 fire events. Additonally, the system flow-balance in Fig A.1 plot shows a pronounced production/consumption surge over the same period as both sources respond.

Compared with the single-fire scenarios, this concurrent-fire case is more severe because it produces a higher count of vulnerable nodes and a larger magnitude in pressure and flow rate deficits. The reason is hydraulic: the J4 fire, at low elevation and close to the tank's influence, pulls strongly from storage, while the J19 fire, at higher elevation, draws from the pump/reservoir side. The two demands load the same conveyance corridor from opposite directions, increasing velocities and head losses, and depressing the hydraulic grade line throughout the spine and the eastern branch. In short, concurrent fires engage both supply sources simultaneously, intensify losses along the trunk, and yield the worst systemwide performance among the three scenarios.

2.3 Synthesis of Findings

The pattern of low pressures follows the ground elevations along the central trunk. With the tank water surface at 71.63 m, the static head available from storage is roughly 41.1 m at J5 (elev. 30.5 m), 22.8 m at J7 (48.8 m), 53.3 m at J4 (18.3 m), and 25.9 m at J19 (45.7 m). Meeting the 2.1-bar requirement requires a hydraulic grade line of elevation + 21.42 m, so J7 and J19 sit close to the threshold (70.22 m and 67.12 m, respectively) and are the first to fall short when the system HGL is pulled down during a fire. J5 and J4 have much larger static cushions and therefore retain service longer for the same upstream head.

Flow routing during the events explains the spatial spread of deficits. In the J5 fire (67–69 h), the event is supplied predominantly from the tank; the central trunk and eastern limb experience elevated velocities and head losses, and at the most vulnerable hour (70), 26 junctions fail both the pressure and demand criteria. In the J7 fire at the same hours, the pump–reservoir side carries most of the load because the elevation and headloss from the tank to J7 are higher; the vulnerability count is again 26, and the same trunk–eastern corridor shows the largest shortfalls, but the storage facility is not the principal supplier. With two concurrent fires at J4 and J19, both sources engage at once: J4 pulls strongly from storage while J19 is fed by the pump. This is why head losses compound in both directions along the trunk. The result is a wider and deeper system-wide depression of the hydraulic grade line, with 29 vulnerable nodes at hour 70 and markedly more negative pressures and delivered-demand deficits than in either single-fire case.

Storage behavior and system flow balance in Fig A.1 and Fig A.3 corroborate this interpretation. The J5 run shows a pronounced tank outflow trough during hours 67–69 and a large post-event refill spike. The J7 run shows little tank draw during the fire window because production from the pump–reservoir meets the event, and its prominent spike near hour 36 reflects routine tank cycling unrelated to the fire. The concurrent J4 & J19 case shows clear tank participation during 67–69 and

strong production/consumption surges in the flow-balance plot as both sources respond simultaneously. Pressure time series at representative trunk nodes reach their minima at hour 70 in all three cases, aligning with the node tables that report the largest counts of junctions below 21.42 m and with delivered demand below 18.37 L/s at that hour. To illustrate why hour 70 (right after the fire event) is the most vulnerable (or the minima), consider hour 71 which is 2 hours after the fire event at hour 69 (Fig. A.6). The number of vulnerable junctions remains 26, yet a comparison with hour 70 (Fig. A.4) shows higher nodal pressures at many locations, indicating ongoing re-pressurization; the count has not fallen because several nodes are still just below the 21.42 m threshold.

Additionally, across all scenarios (as shown in Fig A.5, including the baseline with no fire, the tank pressure (J26) trace is essentially identical because it's just the water depth above the tank bottom. The tank drops rapidly from approximately 21 m to its minimum operating depth (approx. 0.3 m) by about hour 10 and then remains pinned there with small refill bumps, so the later fire window (hrs 67–69) cannot depress it further. Scenario differences, therefore, appear in tank flows and system node pressures, not in the tank's gauge pressure. This indicates the system is effectively pump-dominated during the critical period.

3 Recommendation

The analysis above shows a consistent failure pattern: pressures collapse along the central trunk and the eastern limb, with the lowest values at the end of each three-hour fire (approximately hour 70). Single-fire events at J5 or J7 leave about 26 junctions below both the 21.42 m (2.1 bar) pressure threshold and the scaled demand, while concurrent fires at J4 and J19 cause wider and deeper deficits (about 29 junctions). Elevation explains which locations fail first (higher areas near J7 and J19 sit close to the minimum requirement) while hydraulics explain when and where the collapses occur: long, high-velocity paths along the trunk amplify friction losses precisely when head is most scarce. Compounding this, the tank spends much of the simulation pinned near its minimum operating level, so fires are largely pump-dominated and storage offers limited buffering.

A practical strategy is to create head where it is needed and cut losses where they accumulate, beginning with operations. Raising and widening the tank operating band, and deliberately pre-filling before high-risk periods, restores usable storage so each meter of added level lifts pressures system-wide. Event-based pump controls (for example, pressure-setpoint or critical-node logic) with staged or variable-speed pumping can add head during the three-hour window that governs the worst outcomes. Hydrant protocols that favor hydrants closer to the trunk, or split the 126 L/s between two hydrants, shorten high-loss paths and lower trunk velocities during an event. These operational changes directly improve reliability (share of nodes meeting 21.42 m), adequacy (fraction of demand served), and recovery time, with modest cost and rapid implementation.

Targeted capital upgrades address the corridor that fails first. Upsizing pipes on the central spine and eastern limb and closing key loops reduces friction during high-flow conditions. A booster pump station located on the upper corridor can lift the hydraulic grade for the high-elevation cluster around J7 and J19, directly countering the elevation deficit highlighted by the scenarios. Strategic placement of pressure-sustaining or check valves can stabilize flow reversals observed during fires. These works raise reliability and adequacy during peaks while adding redundancy; they may increase energy use, but the trade-off is fewer low-pressure nodes and shorter recovery after hour 70.

For a more structural shift, decentralization can insulate the vulnerable high-elevation area. Creating a separate pressure zone for the eastern or upper system with a local elevated or ground-level storage tank and a zone booster shortens fire-flow paths, reduces dependence on the long trunk, and prevents the bidirectional "tug-of-war" seen with concurrent fires. Where feasible, an intertie to a neighboring system provides a contingency supply that caps extreme withdrawals from any single corridor. Finally, increasing effective storage by upsizing the tank, increasing usable setpoints, or both ensures the system enters the fire window with headroom above minimum, so storage can absorb part of the 126 L/s demand without collapsing trunk pressures.

A Appendix

This appendix contains supplementary material, including additional graphs and detailed data tables, to provide a more comprehensive explanation and better visual context for the analysis presented in the main document.

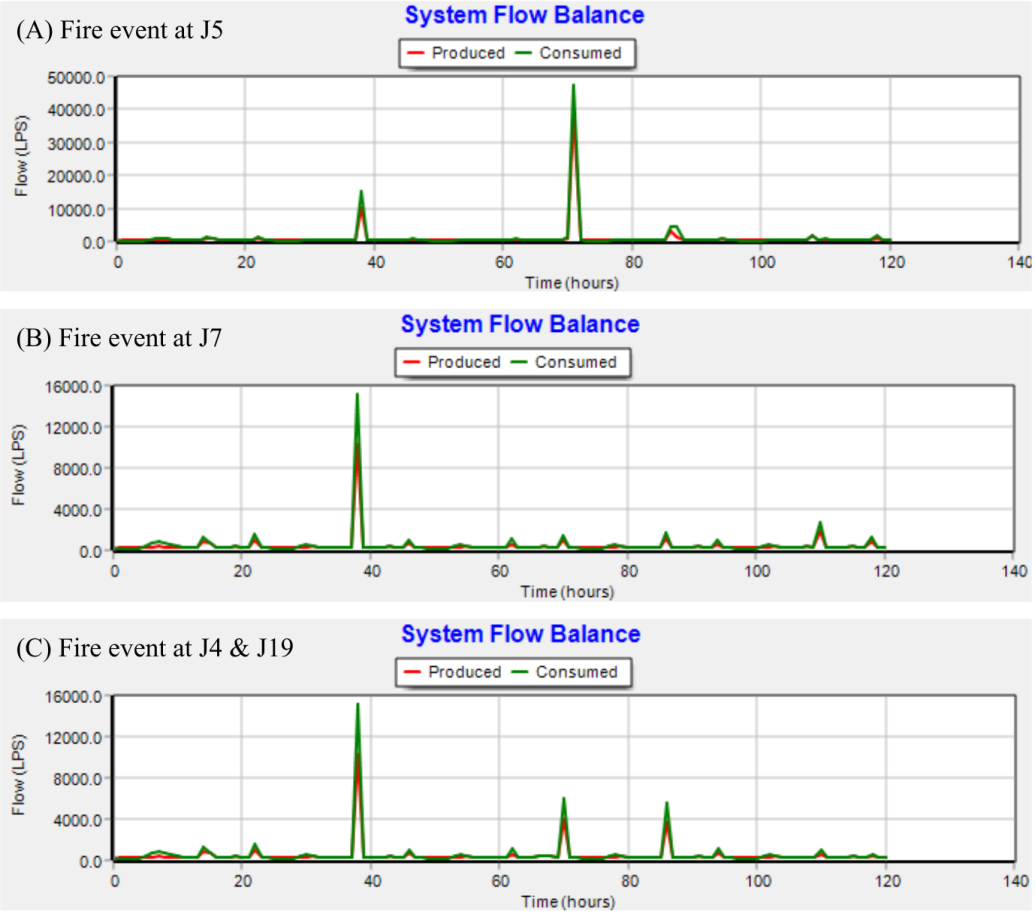

Figure A.1: Comparison of system flow balance (produced vs. consumed) for three fire event scenarios

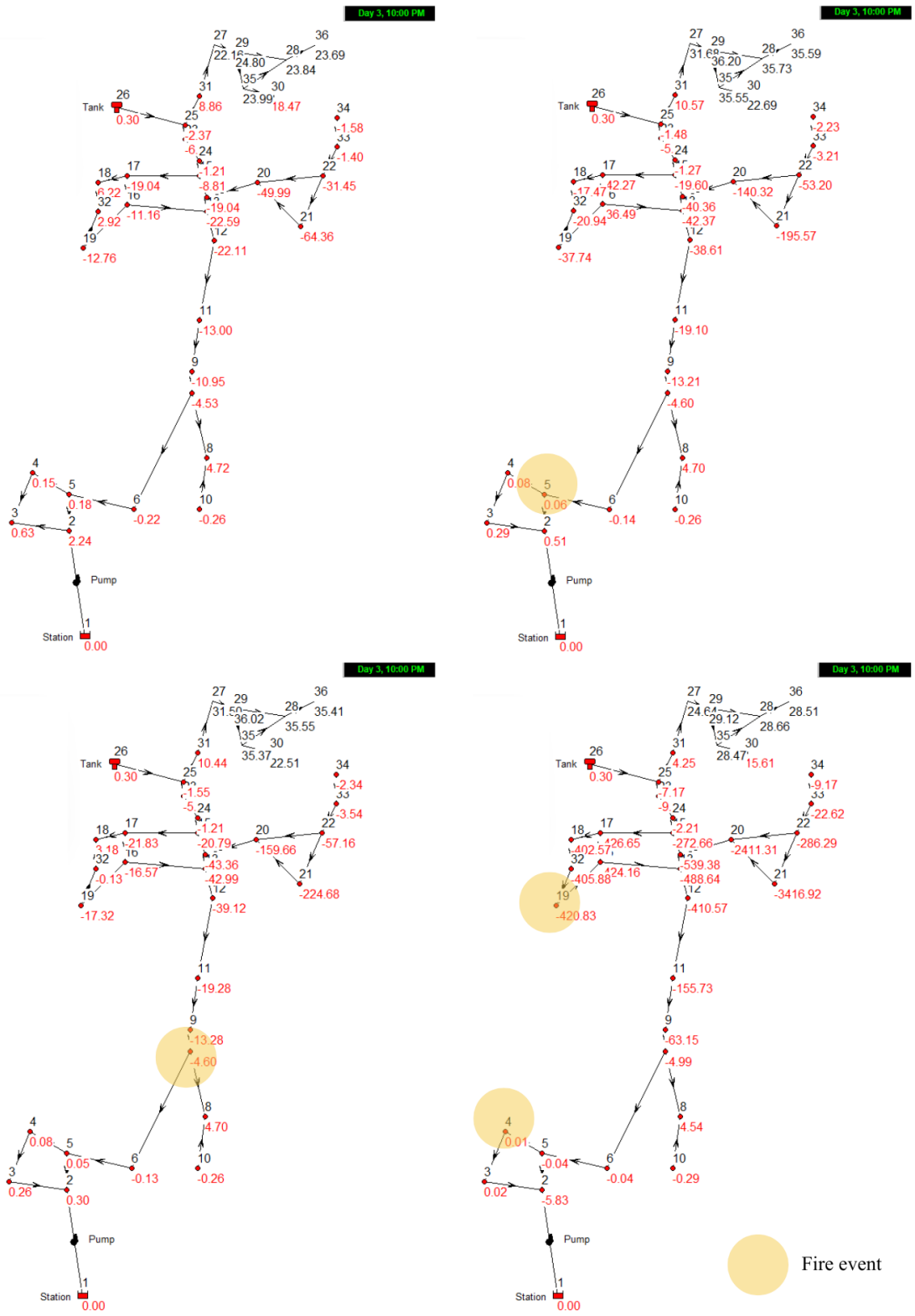

Figure A.2: Four scenarios map on day 3 at 10 PM (70H): baseline (top-left), fire event at J5 (top-right), fire event at J7 (bottom-left), and fire event at J4 and J19 (bottom-right); red texts indicate the nodes with pressure below 21.42 mH2O

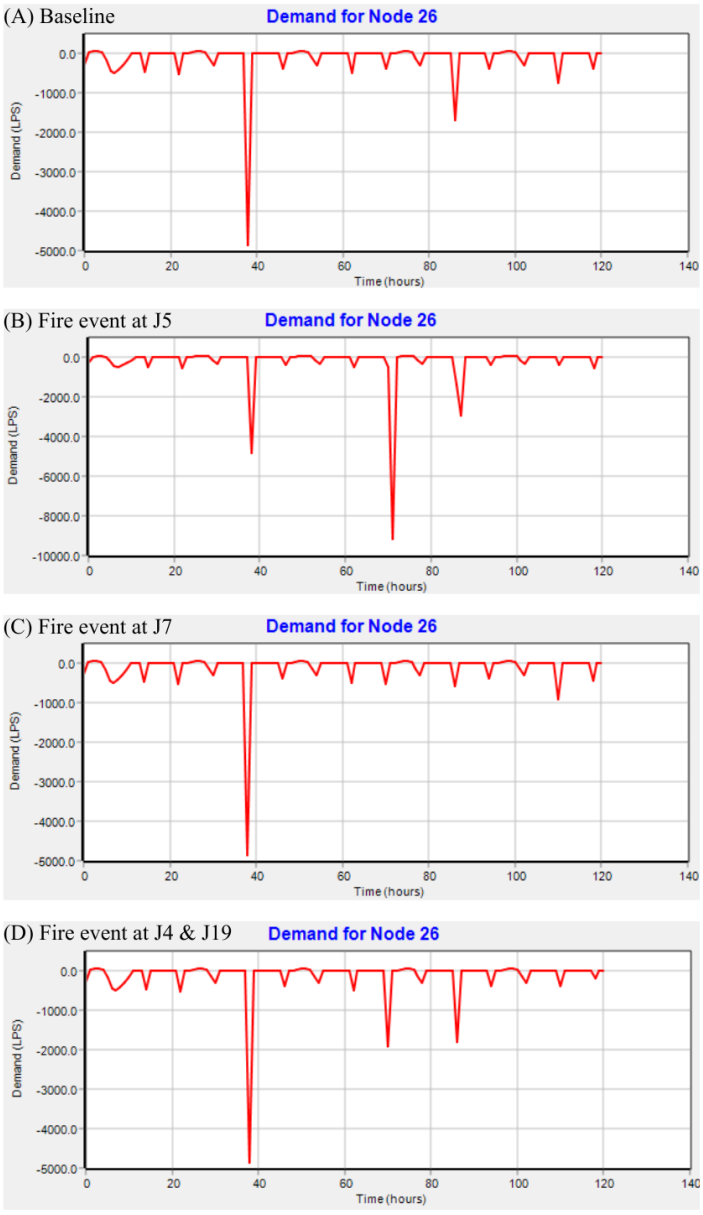

Figure A.3: Comparison of demand over time at the tank (Node 26)

Network Table - Nodes at 70:00 Hrs

Node ID	Demand LPS	Head m	Pressure m
Junc 4	12.97	18.38	0.08
Junc 5	11.52	30.56	0.06
Junc 6	-2.90	37.96	-0.14
Junc 7	-321.70	44.20	-4.60
Junc 9	0.00	41.69	-13.21
Junc 10	-11.61	39.34	-0.26
Junc 11	0.00	37.30	-19.10
Junc 12	0.00	25.39	-38.61
Junc 13	0.00	21.63	-42.37
Junc 14	0.00	20.64	-40.36
Junc 15	0.00	38.30	-19.60
Junc 16	0.00	9.21	-36.49
Junc 17	0.00	12.63	-42.27
Junc 18	14.29	13.03	-17.47
Junc 19	0.00	7.96	-37.74
Junc 20	0.00	-88.52	-140.32
Junc 21	0.00	-149.87	-195.57
Junc 22	0.00	7.80	-53.20
Junc 23	0.00	64.62	-5.48
Junc 24	-213.76	56.63	-1.27
Junc 25	0.00	68.62	-1.48
Junc 31	0.00	68.47	10.57
Junc 32	14.29	12.56	-20.94
Junc 33	-222.09	51.69	-3.21
Junc 34	-151.91	55.67	-2.23
Tank 26	-503.56	71.93	0.30

26 items with
Pressure Below 21.42
Demand Below 18.37

(A) Fire event at J5

Network Table - Nodes at 70:00 Hrs

Node ID	Demand LPS	Head m	Pressure m
Junc 4	12.51	18.38	0.08
Junc 5	10.81	30.55	0.05
Junc 6	-2.32	37.97	-0.13
Junc 7	-321.42	44.20	-4.60
Junc 9	0.00	41.62	-13.28
Junc 10	-11.59	39.34	-0.26
Junc 11	0.00	37.12	-19.28
Junc 12	0.00	24.88	-39.12
Junc 13	0.00	21.01	-42.99
Junc 14	0.00	17.64	-43.36
Junc 15	0.00	37.11	-20.79
Junc 16	0.00	29.13	-16.57
Junc 17	0.00	33.07	-21.83
Junc 18	14.29	33.68	3.18
Junc 19	0.00	28.38	-17.32
Junc 20	0.00	-107.86	-159.66
Junc 21	0.00	-178.98	-224.68
Junc 22	0.00	3.84	-57.16
Junc 23	0.00	64.60	-5.50
Junc 24	-218.64	56.69	-1.21
Junc 25	0.00	68.55	-1.55
Junc 31	0.00	68.34	10.44
Junc 32	-3.80	33.37	-0.13
Junc 33	-245.65	51.36	-3.54
Junc 34	-160.34	55.56	-2.34
Tank 26	-528.25	71.93	0.30

26 items with
Pressure Below 21.42
Demand Below 18.37

(B) Fire event at J7

Network Table - Nodes at 70:00 Hrs

Node ID	Demand LPS	Head m	Pressure m
Junc 2	-409.67	24.67	-5.83
Junc 3	8.92	18.32	0.02
Junc 4	8.02	18.31	0.01
Junc 5	4.54	30.46	-0.04
Junc 6	4.19	38.06	-0.04
Junc 7	-349.68	43.81	-4.99
Junc 9	0.00	-8.25	-63.15
Junc 10	-13.57	39.31	-0.29
Junc 11	0.00	-99.33	-155.73
Junc 12	0.00	-346.57	-410.57
Junc 13	0.00	-424.64	-488.64
Junc 14	0.00	-478.38	-539.38
Junc 15	0.00	-214.76	-272.66
Junc 16	0.00	-378.46	-424.16
Junc 17	0.00	-371.75	-426.65
Junc 18	14.29	-372.07	-402.57
Junc 19	0.00	-375.13	-420.83
Junc 20	0.00	-2359.51	-2411.31
Junc 21	0.00	-3371.22	-3416.92
Junc 22	0.00	-225.29	-286.29
Junc 23	0.00	60.52	-9.58
Junc 24	-1011.46	55.69	-2.21
Junc 25	0.00	62.93	-7.17
Junc 30	0.00	55.21	15.61
Junc 31	0.00	62.15	4.25
Junc 32	0.00	-372.38	-405.88
Junc 33	-1615.48	32.28	-22.62
Junc 34	-650.47	48.73	-9.17
Tank 26	-1921.17	71.93	0.30

29 items with
Pressure Below 21.42
Demand Below 18.37

(C) Fire event at J4 & J19

Figure A.4: Lists of vulnerable nodes with pressure below 21.42 mH2O and demand below their usual value at 70H

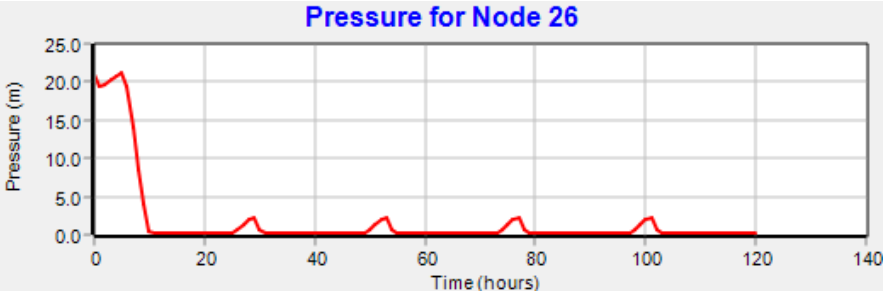

Figure A.5: Pressure at the tank (Node 26) over time - Base case and 3 Fire Scenarios

Network Table - Nodes at 71:00 Hrs

Node ID	Demand LPS	Head m	Pressure m
Junc 11	10.21	75.55	19.15
Junc 12	7.22	64.05	0.05
Junc 13	0.00	60.71	-3.29
Junc 14	0.00	59.05	-1.95
Junc 15	10.20	58.32	0.42
Junc 16	10.21	53.77	8.07
Junc 17	0.00	53.72	-1.18
Junc 19	10.21	53.57	7.87
Junc 20	10.21	58.71	6.91
Junc 21	10.21	58.30	12.60
Junc 22	0.00	58.29	-2.71
Junc 23	0.00	57.39	-12.71
Junc 24	9.82	57.99	0.09
Junc 25	0.00	57.10	-13.00
Junc 27	10.21	53.63	14.03
Junc 28	10.21	51.02	17.52
Junc 29	10.21	51.58	18.08
Junc 30	10.21	50.77	11.17
Junc 31	0.00	56.50	-1.40
Junc 32	10.21	53.59	20.09
Junc 33	10.21	57.91	3.01

26 items with
Pressure Below 21.42

Figure A.6: Demonstration of water pressure and demand at hour 71 after fire event at J5